I&EC research
Industrial & Engineering Chemistry Research
pubs.acs.org/IECR
Article

Design Optimization of Double-Pipe Heat Exchangers Using a Discretized Model

André L. M. Nahes, Miguel J. Bagajewicz, and André L. H. Costa*

Cite This: *Ind. Eng. Chem. Res.* 2021, 60, 17611−17625
Read Online
ACCESS | Metrics & More | Article Recommendations | Supporting Information

ABSTRACT: The design optimization of heat exchangers is a topic extensively investigated in the literature. The majority of the papers that addressed this problem employed closed-form analytical solutions to describe the behavior of the equipment, such as the logarithmic mean temperature difference (LMTD) and effectiveness (ε-NTU) methods. These analytical solutions are based on the hypothesis of uniform values of the physical properties and heat transfer coefficients. This assumption may imply considerable errors in several situations. Aiming at eliminating these limitations, we present a novel integer linear model for the optimal design of hairpin double-pipe heat exchangers. Our novel method discretizes the temperature field inside the exchangers and, together with appropriate rigorous reformulations, renders a linear model. Numerical results illustrate the performance of the proposed approach, showing that the analytical solutions can significantly undersize or oversize the heat exchanger.

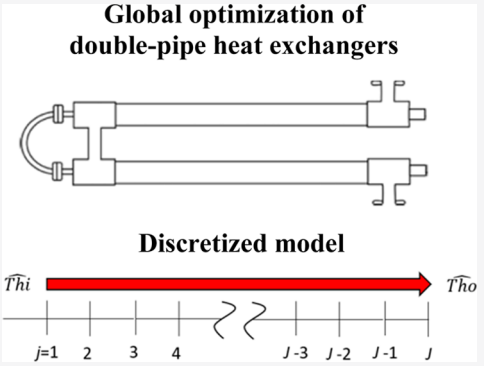

1. INTRODUCTION

The capital cost of thermal equipment corresponds to a considerable fraction of the total investment in new projects of chemical process industries. Therefore, there is an intense effort in the literature for the development of solutions for the design optimization of heat exchangers. Almost all papers that addressed this design optimization problem employed mathematical models based on analytical solutions, such as the logarithmic mean temperature difference method (LMTD) or the effectiveness method (ε-NTU). Table 1 presents a set of references that addressed the design optimization of different kinds of heat exchangers using these methods.

Table 1. References of Heat Exchanger Design Using Analytical Solutions

type of heat exchanger	LMTD	ε-NTU
shell-and-tube	1	2
double-pipe	3	4
air cooler	5	6
gasketed plate	7	8
plate-fin	9	10

Other kinds of analytical solutions were also explored in the design optimization algorithms. For example, Mota et al.[11] employed a linear set of ordinary differential equations for the design optimization of gasketed plate heat exchangers. The utilization of models based on analytical solutions is also prevalent in problems involving heat exchanger network synthesis (HENS), where the LMTD method is used.[12]

The analytical solutions of heat exchanger design problems are derived assuming uniform values of the overall heat transfer coefficient and stream heat capacities, which is associated with the assumption of constant values for the physical properties of the fluids.[13] However, there are streams associated with large variations of the physical properties and the utilization of the assumption of uniform physical properties in these cases can bring large deviations from reality. This potential problem and the need for higher accuracy explain the fact that professional engineering software for the design and rating of heat exchangers does not use analytical solutions (e.g., HTRI XIST and Aspen Exchanger Design and Rating EDR). These programs are based on a discretization of the heat transfer equations.[14] In fact, several papers addressed the simulation of heat exchangers through discretization techniques[15] or even computational fluid dynamics.[16] Recently, heat exchanger models associated with numerical discretization procedures have also been used for the design optimization[17] and heat exchanger network synthesis.[18,19]

The limitations exposed above of the closed-form analytical solutions hinder the utilization of design optimization tools for engineering practice.[20] Therefore, this paper discusses the optimization of heat exchangers based on models where the

Received: June 24, 2021
Revised: October 11, 2021
Accepted: November 4, 2021
Published: November 23, 2021

https://doi.org/10.1021/acs.iecr.1c02455
Ind. Eng. Chem. Res. 2021, 60, 17611−17625

physical properties and the heat transfer coefficients vary along the heat transfer surface. Particularly, this paper addresses the design optimization of double-pipe heat exchangers. The heat exchanger model is based on the discretization of the differential equations of the energy balance, where the physical properties are evaluated at each point of the resultant grid. Additionally, a mechanical energy balance is also employed in the model for the determination of the pressure drop throughout the heat exchanger. Instead of discretizing the domain using the spatial coordinate, as it is usual in transport phenomena problems, the proposed approach applies a discretization of the temperature field as the independent variable. This representation of the problem associated with proper mathematical transformations yields a linear problem. The global optimum of the problem can be obtained using integer linear programming (ILP). The linearity of the formulation eliminates convergence problems, the need for good initial estimates, or the presence of multiple local optima with different values of the objective function.

The remainder of the paper is organized as follows. Section 2 presents the mathematical model of the heat exchanger, Section 3 presents the discretization of the differential model yielding an algebraic set of equations, Section 4 presents a formulation of the design optimization problem using the heat exchanger discretized model, Section 5 shows how the optimization model can be reformulated in a linear form, Section 6 depicts the numerical results, and Section 7 presents the conclusions.

2. SYSTEM MODEL

2.1. System Investigated. The proposed approach is applied to a system consisting of double-pipe heat exchangers. This kind of thermal equipment is composed of two concentric tubes, where one of the streams flows inside the inner tube and the other flows in the annulus formed by the space between the inner and outer tubes (there are variants of this structure where the inner tube is substituted by a small tube bundle).[21]

Typical double-pipe heat exchangers are composed of hairpins, as illustrated in Figure 1.

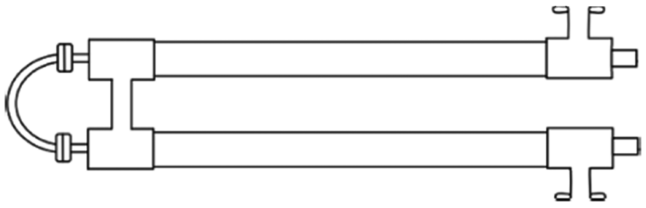

Figure 1. Hairpins.

The design variables of a hairpin are the outer and inner diameters of the inner tube (*dte* and *dti*), the outer and inner diameters of the outer tube (*Dte* and *Dti*), and the hairpin tube length (*Lh*). The tube thickness is assumed previously known; therefore, the diameters of the inner and outer tubes are only associated with two degrees of freedom. The tube length of a hairpin corresponds to the sum of the lengths of the two interconnected pairs of tubes.

Double-pipe heat exchangers are modular structures that can be organized in different arrangements. In this paper, a set of hairpins connected in series are called a unit and it is possible to connect several units in parallel, i.e., each unit corresponds to a branch of the structure. The number of hairpins connected in series in a unit and the number of parallel branches are design variables represented by NS and NB, respectively.

Figure 2 illustrates a structure composed of two parallel branches; the units of each branch are composed of three hairpins.

2.2. Heat Exchanger Model. The heat exchanger model corresponds to a set of differential equations related to the energy and mechanical energy balances. Turbulent flow is assumed ($Re > 4000$) since this is a regime usually observed in industrial practice. The control volume is represented in Figure 3, considering a pipe section of the hairpin in the countercurrent flow (without loss of generality, the hot fluid flows in the annulus), where the inlet/outlet temperatures of the hot and cold streams in the heat exchanger are $\widehat{Thi}/\widehat{Tho}$ and $\widehat{Tci}/\widehat{Tco}$, respectively. In the presentation of the model below, the parameters are identified with a symbol $\wedge$ on top (e.g., the inlet and outlet temperatures are problem parameters, according to the thermal task).

The energy balance for both streams can be represented by the following system of differential equations[13]

$$\frac{dT_h}{dz} = -\frac{U(T_h - T_c)\pi dte}{(\hat{m}_h/NB)Cp_h} \tag{1}$$

$$\frac{dT_c}{dz} = -\frac{U\ (T_h - T_c)\pi dte}{(\hat{m}_c/NB)\ Cp_c} \tag{2}$$

where T is the stream temperature, z is the spatial coordinate, U is the overall heat transfer coefficient, $\hat{m}$ is the stream mass flow rate, Cp is the heat capacity, and the subscripts h and c represent the hot and cold streams, respectively. The conduction along the flow direction and the variations of the kinetic and potential energies are dismissed in eqs 1 and 2 because they are usually negligible in heat exchanger problems.

The corresponding boundary conditions are

$$T_h|_{z=0} = \widehat{Thi} \tag{3}$$

$$T_c|_{z=L} = \widehat{Tci} \tag{4}$$

The expression of the overall heat transfer is given by

$$U = \frac{1}{\frac{1}{h_c}\left(\frac{dte}{dti}\right) + \widehat{Rf}_c\left(\frac{dte}{dti}\right) + \frac{dte\ \ln\left(\frac{dte}{dti}\right)}{2\hat{k}_{tube}} + \widehat{Rf}_h + \frac{1}{h_h}} \tag{5}$$

where $\hat{k}_{tube}$ is the thermal conductivity of the inner tube, h is the convective heat transfer coefficient, and $\widehat{Rf}$ is the fouling factor. The convective heat transfer coefficients are calculated using the Gnielinski correlation (see the Supporting Information).[13]

The mechanical energy balance written in the differential form is given by (assuming that the heat exchanger is placed in a horizontal position)

$$\frac{1}{\rho_c}\frac{dP_c}{dz} + v_c\frac{dv_c}{dz} = \frac{dF_c}{dz} \tag{6}$$

$$\frac{1}{\rho_h}\frac{dP_h}{dz} + v_h\frac{dv_h}{dz} = \frac{dF_h}{dz} \tag{7}$$

where P is the pressure and F is the mechanical energy loss associated with friction. According to the Darcy–Weisbach equation[21]

$$\frac{dF_c}{dz} = f_c\frac{v_c^2}{2dti} \tag{8}$$

https://doi.org/10.1021/acs.iecr.1c02455
Ind. Eng. Chem. Res. 2021, 60, 17611−17625

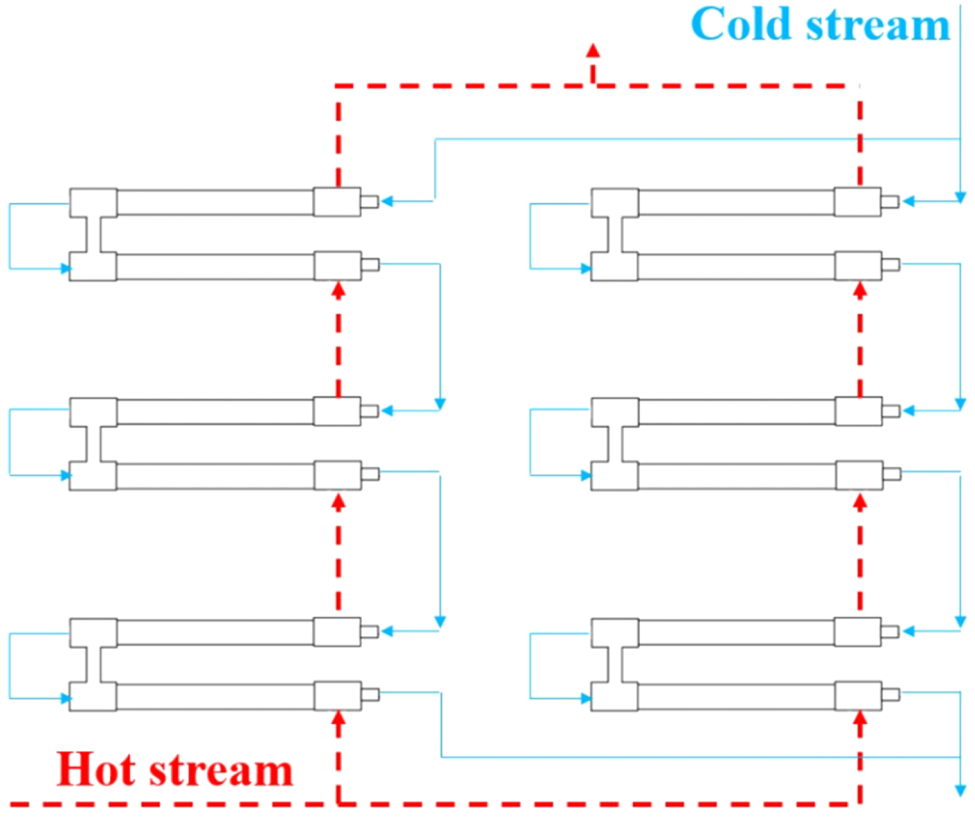

Figure 2. Two parallel branches with units containing three hairpins in series.

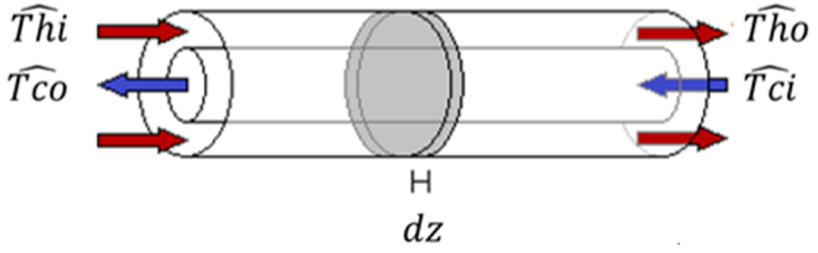

Figure 3. Control volume employed in the modeling of a double-pipe heat exchanger.

$$\frac{dF_h}{dz} = -f_h \frac{v_h^2}{2dh} \tag{9}$$

The Darcy friction factor in eqs 8 and 9 can be calculated using the relations presented in Saunders (see the Supporting Information).[21]

The flow velocity of the cold stream in the tube side and the hot stream in the annulus are given by

$$v_c = \frac{\widehat{m_c}/\rho_c}{NB\ As_c} \tag{10}$$

$$v_h = \frac{\widehat{m_h}/\rho_h}{NB\ As_h} \tag{11}$$

where the cross-sectional areas, As_c and As_h, are calculated as follows

$$As_c = \frac{\pi dti^2}{4} \tag{12}$$

$$As_h = \frac{\pi}{4}(Dti^2 - dte^2) \tag{13}$$

It is important to observe that the physical properties presented in the above equations depend on the temperature (effects related to pressure variations are not considered in the model)

$$\rho = \rho(T) \tag{14}$$

$$Cp = Cp(T) \tag{15}$$

$$\mu = \mu(T) \tag{16}$$

$$k = k(T) \tag{17}$$

Consequently, for a given set of design variables, the overall heat transfer coefficient is dependent on the temperatures of the streams

$$U = U(T_h, T_c) \tag{18}$$

3. DISCRETIZED MODEL

The model described above is composed of a system of four nonlinear differential equations. Considering that the design problem establishes fixed inlet and outlet temperatures, the proposed formulation is based on an inversion of the

https://doi.org/10.1021/acs.iecr.1c02455
Ind. Eng. Chem. Res. 2021, 60, 17611−17625

conventional representation of the model. The discretization of the set of differential equations is not based on a spatial grid, as it is usual in problems of transport phenomena, but in a thermal grid, where the stream temperature along the heat exchanger is assumed known and the spatial coordinate is the unknown variable.

3.1. Discretization Procedure Based on a Temperature Grid. According to this representation, a temperature grid for the hot stream is established, associated with an index $j = 1, ..., J$,

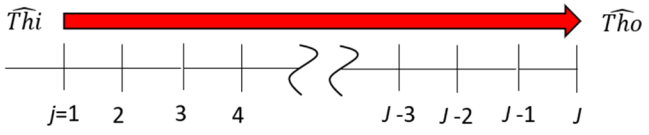

Figure 4. Hot-stream temperature grid.

as presented in Figure 4. The thermal grid is coupled to the design specifications

$$\hat{T}_{h,j} = \widehat{Thi} \quad \text{for } j = 1 \tag{19}$$

$$\hat{T}_{h,j} = \hat{T}_{h,j-1} + \widehat{\Delta T_h} \quad \text{for } j = 2, ..., J \tag{20}$$

$$\widehat{\Delta T_h} = \frac{\widehat{Tho} - \widehat{Thi}}{\hat{J} - 1} \tag{21}$$

The energy balances imply that the temperatures of the cold stream associated with the grid of the hot-stream temperatures can be calculated directly. The division of eq 2 by eq 1 yields the following relation between the hot and cold stream temperatures along the length of the heat exchanger

$$\frac{dT_c}{dT_h} = \frac{\widehat{m_h} Cp_h}{\widehat{m_c} Cp_c} \tag{22}$$

The corresponding boundary condition is

$$T_c|_{T_h = \widehat{Tho}} = \widehat{Tci} \tag{23}$$

The application of the midpoint discretization procedure generates the following numerical approximation of eq 22

$$\frac{T_{c,j} - T_{c,j-1}}{\widehat{\Delta T_h}} = \frac{\widehat{m_h}\ \widehat{Cp}_{h,j-1/2}}{\widehat{m_c} Cp_{c,j-1/2}} \quad \text{for } j = 2, ..., J \tag{24}$$

Additionally, eq 23 yields

$$T_{c,j} = \widehat{Tci} \quad \text{for } j = J \tag{25}$$

The heat capacities in eq 24, $\widehat{Cp}_{h,j-1/2}$ and $Cp_{c,j-1/2}$, correspond to the evaluation of their values as follows

$$\widehat{Cp}_{h,j-1/2} = Cp_h\left(\frac{\hat{T}_{h,j} + \hat{T}_{h,j-1}}{2}\right) = Cp_h\left(\hat{T}_{h,j-1} + \frac{\widehat{\Delta T_h}}{2}\right) \tag{26}$$

$$Cp_{c,j-1/2} = Cp_c\left(\frac{T_{c,j} + T_{c,j-1}}{2}\right) \tag{27}$$

The system of equations represented by eqs 24−27 can be solved to yield the cold-stream temperatures along the grid. Therefore, because the cold-stream temperatures are calculated before the optimization, from now on, they will be considered as parameters.

According to the proposal of a thermal grid, the differential equation of the energy balance for the hot stream in eq 1 is reorganized as follows

$$\frac{dz}{dT_h} = -\frac{(\hat{m}_h/NB)\ Cp_h}{U(T_h - T_c)\ \pi\ dte} \tag{28}$$

where the boundary condition is

$$z|_{T_h = \widehat{Thi}} = 0 \tag{29}$$

The midpoint discretization technique is then applied to the differential model, thus yielding

$$\frac{z_j - z_{j-1}}{\widehat{\Delta T_h}} = -\frac{\hat{m}_h\ \widehat{Cp}_{h,j-1/2}}{\hat{U}_{j-1/2}(\hat{T}_{h,j-1/2} - \hat{T}_{c,j-1/2})\pi\ dte\ NB} \quad \text{for } j = 2, ..., J \tag{30}$$

where the temperatures and the overall heat transfer coefficient at the midpoints of the grid $(j - 1/2)$ correspond to

$$\hat{T}_{h,j-1/2} = \frac{\hat{T}_{h,j} + \hat{T}_{h,j-1}}{2} = \hat{T}_{h,j-1} + \frac{\widehat{\Delta T_h}}{2} \tag{31}$$

$$\hat{T}_{c,j-1/2} = \frac{\hat{T}_{c,j} + \hat{T}_{c,j-1}}{2} \tag{32}$$

$$\hat{U}_{j-1/2} = U\left(\hat{T}_{h,j-1} + \frac{\widehat{\Delta T_h}}{2}, \hat{T}_{c,j-1} + \frac{\widehat{\Delta T_h}}{2}\right) \tag{33}$$

The corresponding boundary condition becomes

$$z|_{j=1} = 0 \tag{34}$$

In this representation, the temperatures became fixed parameters and, therefore, the physical properties too, evaluated through relations expressed in eqs 14−17. Additionally, for a given set of design variables, the overall heat transfer coefficient also becomes a parameter, calculated using the heat transfer correlations based on the stream physical properties evaluated at each point of the grid.

The mechanical energy balances are also reorganized according to the thermal grid proposal, and then eqs 8−11 are substituted into eqs 6 and 7, and the results are multiplied by $\rho_c^2(dz/dT_h)$ and $\rho_h^2(dz/dT_h)$, respectively

$$\rho_c \frac{dP_c}{dT_h} - \left(\frac{\widehat{m_c}}{NB\ As_c}\right)^2\left(\frac{1}{\rho_c}\right)\frac{d\rho_c}{dT_h} - \left(\frac{\hat{m}_c}{NBAs_c}\right)^2 \frac{f_c}{2dti}\frac{dz}{dT_h} = 0 \tag{35}$$

$$\rho_h \frac{dP_h}{dT_h} - \left(\frac{\hat{m}_h}{NB\ As_h}\right)^2\left(\frac{1}{\rho_h}\right)\frac{d\rho_h}{dT_h} + \left(\frac{\hat{m}_h}{NB\ As_h}\right)^2 \frac{f_h}{2dh}\frac{dz}{dT_h} = 0 \tag{36}$$

Let β be the coefficient of thermal expansion[13]

$$\beta = -\left(\frac{1}{\rho}\right)\frac{d\rho}{dT} \tag{37}$$

Therefore, eqs 35 and 36 are equivalent to

https://doi.org/10.1021/acs.iecr.1c02455
Ind. Eng. Chem. Res. 2021, 60, 17611−17625

$$\rho_c \frac{dP_c}{dT_h} + \left(\frac{\hat{m}_c}{NB\ As_c}\right)^2 \beta_c \frac{dT_c}{dT_h} - \left(\frac{\hat{m}_c}{NB\ As_c}\right)^2 \frac{f_c}{2dti} \frac{dz}{dT_h} = 0 \tag{38}$$

$$\rho_h \frac{dP_h}{dT_h} + \left(\frac{\hat{m}_h}{Nb\ As_h}\right)^2 \beta_h + \left(\frac{\hat{m}_h}{Nb\ As_h}\right)^2 \frac{f_h}{2dh} \frac{dz}{dT_h} = 0 \tag{39}$$

Using the midpoint method, the mechanical energy balances become

$$\hat{\rho}_{c,j-1/2}\left(\frac{P_{c,j} - P_{c,j-1}}{\widehat{\Delta T_h}}\right) + \left(\frac{\hat{m}_c}{NB\ As_c}\right)^2 \hat{\beta}_{c,j+1/2} \frac{\widehat{m_h}\ \widehat{Cp}_{h,j-1/2}}{\widehat{m_c}\widehat{Cp}_{c,j-1/2}} - \left(\frac{\hat{m}_c}{NB\ As_c}\right)^2 \frac{f_{c,j-1/2}}{2dti}\left(\frac{z_j - z_{j-1}}{\widehat{\Delta T_h}}\right) = 0 \text{ for } j = 2, ..., J \tag{40}$$

$$\hat{\rho}_{h,j-1/2}\left(\frac{P_{h,j} - P_{h,j-1}}{\widehat{\Delta T_h}}\right) + \left(\frac{\hat{m}_c}{NB\ As_h}\right)^2 \hat{\beta}_{h,j+1/2} + \left(\frac{\hat{m}_h}{NB\ As_h}\right)^2 \frac{f_{h,j-1/2}}{2dh}\left(\frac{z_j - z_{j-1}}{\widehat{\Delta T_h}}\right) = 0 \text{ for } j = 2, ..., J \tag{41}$$

The boundary conditions are

$$P_{c,j=J} = \widehat{Pci} \tag{42}$$

$$P_{h,j=1} = \widehat{Phi} \tag{43}$$

where $\widehat{Phi}$ and $\widehat{Pci}$ are the inlet pressure of hot and cold streams, respectively.

The difference $z_J - z_1$ is equivalent to the required tube length for a given thermal task and can be calculated by the summation of the discretized energy balances represented in eq 30

$$z_J - z_1 = -\widehat{\Delta T_h} \sum_{j=2}^{J} \frac{\hat{m}_h\ \widehat{Cp}_{h,j-1/2}}{\hat{U}_{j-1/2}(\hat{T}_{h,j-1/2} - \hat{T}_{c,j-1/2})\pi\ dte\ NB} \tag{44}$$

The differences $P_{h,J} - P_{h,1}$ and $P_{c,1} - P_{c,J}$ correspond to the hot- and cold-stream pressure drops and can be calculated through the mechanical energy balances, as follows.

The difference between z_j and z_{j-1} in eq 30 can be substituted into the mechanical energy balances in eqs 40 and 41, thus obtaining

$$\hat{\rho}_{c,j-1/2}\left[\frac{P_{c,j} - P_{c,j-1}}{\widehat{\Delta T_h}}\right] + \left(\frac{\hat{m}_c}{NB\ As_c}\right)^2 \hat{\beta}_{c,j+1/2} \frac{\widehat{m_h}\ \widehat{Cp}_{h,j-1/2}}{\widehat{m_c}\widehat{Cp}_{c,j-1/2}} + \left(\frac{\hat{m}_c}{NB\ As_c}\right)^2 \frac{\hat{f}_{c,j-1/2}}{2dti}\left[\frac{\hat{m}_h\ \widehat{Cp}_{h,j-1/2}}{\hat{U}_{j-1/2}(\widehat{Th}_{j-1/2} - \widehat{Tc}_{j-1/2})\pi\ dte\ NB}\right] = 0 \text{ for } j = 2, ..., J \tag{45}$$

$$\hat{\rho}_{h,j-1/2}\left[\frac{P_{h,j} - P_{h,j-1}}{\widehat{\Delta T_h}}\right] + \left(\frac{\hat{m}_h}{NB\ As_h}\right)^2 \hat{\beta}_{h,j+1/2} - \left(\frac{\hat{m}_h}{NB\ As_h}\right)^2 \frac{\hat{f}_{h,j-1/2}}{2dh}\left[\frac{\hat{m}_h\ \widehat{Cp}_{h,j-1/2}}{\hat{U}_{j-1/2}(\widehat{Th}_{j-1/2} - \widehat{Tc}_{j-1/2})\pi\ dte\ NB}\right] = 0 \text{ for } j = 2, ..., J \tag{46}$$

The summation of eqs 45 and 46 yields the corresponding expressions of the pressure drops

$$P_{c,J} - P_{c,1} = \sum_{j=2}^{J} \frac{-\widehat{\Delta T_h}}{\hat{\rho}_{c,j-1/2}}\left\{\left(\frac{\hat{m}_c}{NB\ As_c}\right)^2 \hat{\beta}_{c,j+1/2} \frac{\widehat{m_h}\ \widehat{Cp}_{h,j-1/2}}{\widehat{m_c}\widehat{Cp}_{c,j-1/2}} + \left(\frac{\hat{m}_c}{NB\ As_c}\right)^2 \frac{f_{c,j-1/2}}{2dti}\left[\frac{\hat{m}_h\ \widehat{Cp}_{h,j-1/2}}{\hat{U}_{j-1/2}(\widehat{Th}_{j-1/2} - \widehat{Tc}_{j-1/2})\pi\ dte\ NB}\right]\right\} \tag{47}$$

$$P_{h,1} - P_{h,J} = \sum_{j=2}^{J} \frac{\widehat{\Delta T_h}}{\hat{\rho}_{h,j-1/2}}\left\{\left(\frac{\hat{m}_h}{NB\ As_h}\right)^2 \hat{\beta}_{h,j+1/2} - \left(\frac{\hat{m}_h}{NB\ As_h}\right)^2 \frac{f_{h,j-1/2}}{2dh}\left[\frac{\hat{m}_h\ \widehat{Cp}_{h,j-1/2}}{\hat{U}_{j-1/2}(\widehat{Th}_{j-1/2} - \widehat{Tc}_{j-1/2})\pi\ dte\ NB}\right]\right\} \tag{48}$$

3.2. Comparison with a Conventional Discretization Procedure. The conventional discretization procedure employed in the solution of transport phenomena problems typically uses a spatial grid. The application of this scheme in the current problem yields the spatial coordinates associated with the grid as problem parameters and the stream temperatures as state variables. In this case, the energy and mechanical balances are represented by

$$\frac{T_{h,j} - T_{h,j-1}}{\widehat{\Delta y}} = -\frac{\overline{U}_j(\overline{T}_{h,j} - \overline{T}_{c,j})\pi\ dte\ NB}{\hat{m}_h\ \overline{Cp}_{h,j}} \quad \text{for } j = 2, ..., J \tag{49}$$

$$\frac{T_{c,j} - T_{c,j-1}}{\widehat{\Delta y}} = -\frac{\overline{U}_j\ (\overline{T}_{h,j} - \overline{T}_{c,j})\pi\ dte}{(\hat{m}_c/NB)\ \overline{Cp}_{c,j}} \quad \text{for } j = 2, ..., J \tag{50}$$

$$\frac{1}{\overline{\rho}_{c,j}} \frac{P_{c,j} - P_{c,j-1}}{\widehat{\Delta y}} + v_{c,j} \frac{v_{c,j} - v_{c,j-1}}{\widehat{\Delta y}} = \overline{f}_{c,j} \frac{v_{c,j}^2}{2dti} \quad \text{for } j = 2, ..., J \tag{51}$$

$$\frac{1}{\overline{\rho}_{h,j}} \frac{P_{h,j} - P_{h,j-1}}{\widehat{\Delta y}} + v_{h,j} \frac{v_{h,j} - v_{h,j-1}}{\widehat{\Delta y}} = -\overline{f}_{h,j} \frac{v_{h,j}^2}{2dh} \quad \text{for } j = 2, ..., J \tag{52}$$

where the average properties and transport coefficients are

$$\overline{T}_{h,j} = \frac{T_{h,j} + T_{h,j-1}}{2} \tag{53}$$

$$\overline{T}_{c,j} = \frac{T_{c,j} + T_{c,j-1}}{2} \tag{54}$$

$$\overline{U}_j = U\left(\frac{T_{h,j} + T_{h,j-1}}{2}, \frac{T_{c,j} + T_{c,j-1}}{2}\right) \tag{55}$$

$$\overline{f}_{c,j} = f_c\left(\frac{T_{c,j} + T_{c,j-1}}{2}\right) \tag{56}$$

$$\overline{f}_{h,j} = f_h\left(\frac{T_{h,j} + T_{h,j-1}}{2}\right) \tag{57}$$

https://doi.org/10.1021/acs.iecr.1c02455
Ind. Eng. Chem. Res. 2021, 60, 17611−17625

$$\overline{Cp}_{h,j} = Cp_h\left(\frac{T_{h,j} + T_{h,j-1}}{2}\right) \quad (58)$$

$$\overline{Cp}_{c,j} = Cp_c\left(\frac{T_{c,j} + T_{c,j-1}}{2}\right) \quad (59)$$

$$\overline{\rho}_{h,j} = \rho_h\left(\frac{T_{h,j} + T_{h,j-1}}{2}\right) \quad (60)$$

$$\overline{\rho}_{c,j} = \rho_c\left(\frac{T_{c,j} + T_{c,j-1}}{2}\right) \quad (61)$$

Considering the variation of the physical properties with the temperature, the transport coefficients (the overall heat transfer coefficient and the friction factor) become nonlinear functions associated with proper correlations. Therefore, the resultant discretized model, represented by eqs 49−60, becomes nonlinear. The utilization of nonlinear models in optimization problems brings several drawbacks, such as nonconvergence issues and the possibility of the presence of multiple local optima with different values of the objective function. The alternative discretization scheme presented here avoids these obstacles, yielding a linear optimization problem, as shown in the next section.

4. OPTIMIZATION PROBLEM

The optimization minimizes the area of the double-pipe heat exchanger, including the complete structure with the hairpins distributed along the different branches and units

$$\min \pi\ dte\ Lh\ NS\ NB + \widehat{ph}\ NS\ NB \quad (62)$$

The second term of the objective function is introduced to avoid multiple solutions with the same area; the penalty factor $\widehat{ph}$ is a small positive number that drives the optimization toward the minimal area solution with the smallest number of hairpins. This can also be done by constraining the number of hairpins successively until the problem is infeasible.

The optimization problem constraints involve the heat exchanger model equations described above, bounds on pressure drop, flow velocity, and hairpin tube length, and an inequality stating that the outer tube diameter is larger than the inner tube diameter.

The number of hairpins in each unit and the tube length of each hairpin must be sufficient to provide the necessary heat transfer rate according to the energy balance, which yields the following constraint

$$Lh\ NS = z_J - z_1 \quad (63)$$

Additionally, the tube length of each hairpin is limited by maximum and minimum values ($\widehat{Lh}^{LB}$ and $\widehat{Lh}^{UB}$)

$$\widehat{Lh}^{LB} \le Lh \le \widehat{Lh}^{UB} \quad (64)$$

The length Lh can be related to the other design variables through the substitution of eq 44 into eq 63

$$Lh = \sum_{j=2}^{J} \frac{-\hat{m}_h\ \widehat{Cp}_{h,j-1/2}\widehat{\Delta T}_h}{U_{j-1/2}(NB,\ dti,\ dte,\ Dti)(\widehat{Th}_{j-1/2} - \widehat{Tc}_{j-1/2})\pi\ dte\ NB\ NS} \quad (65)$$

In this equation, it is expressed that the overall heat transfer coefficient evaluated at each point of the thermal grid in the optimization problem depends on the design variables: number of parallel branches and the diameters of the inner and outer tubes.

Therefore, the variable Lh can be eliminated from the optimization problem through the substitution of eq 65 into the objective function in eq 62 and the constraint of eq 64, thus yielding

$$\min \sum_{j=2}^{J} \frac{-\hat{m}_h\ \widehat{Cp}_{h,j-1/2}\widehat{\Delta T}_h}{U_{j-1/2}(NB,\ dti,\ dte,\ Dti)(\widehat{Th}_{j-1/2} - \widehat{Tc}_{j-1/2})} + \widehat{ph}\ NS\ NB \quad (66)$$

$$\widehat{Lh}^{LB} \le \sum_{j=2}^{J} \frac{-\hat{m}_h\ \widehat{Cp}_{h,j-1/2}\widehat{\Delta T}_h}{U_{j-1/2}(NB,\ dti,\ dte,\ Dti)(\widehat{Th}_{j-1/2} - \widehat{Tc}_{j-1/2})\pi\ dte\ NB\ NS} \le \widehat{Lh}^{UB} \quad (67)$$

The pressure drops are constrained by upper bounds

$$\Delta P_h \le \widehat{\Delta P}_{h,disp} \quad (68)$$

$$\Delta P_c \le \widehat{\Delta P}_{c,disp} \quad (69)$$

where ΔP is the stream pressure drop and $\widehat{\Delta P}_{disp}$ is the corresponding maximum available value. As discussed before, the representations of these constraints according to the discretized model are

$$P_{h,1} - P_{h,J} \le \widehat{\Delta P}_{h_{disp}} \quad (70)$$

$$P_{c,J} - P_{c,1} \le \widehat{\Delta P}_{c_{disp}} \quad (71)$$

The substitutions of eqs 47 and 48 into eqs 70 and 71, including the boundary conditions from eqs 42 and 43, yield (the friction factor also depends on the number of parallel branches and the diameters of the inner and outer tubes)

$$\sum_{j=2}^{J} \frac{\widehat{\Delta T}_h}{\hat{\rho}_{h,j-1/2}}\left\{\left(\frac{\hat{m}_h}{NB\ As_h}\right)^2 \hat{\beta}_{h,j+1/2} - \left(\frac{\hat{m}_h}{NB\ As_h}\right)^2 \frac{f_{h,j-1/2}(NB,\ dti,\ dte,\ Dti)}{2dh}\left[\frac{\hat{m}_h\ \widehat{Cp}_{h,j-1/2}}{U_{j-1/2}(NB,\ dti,\ dte,\ Dti)(\widehat{Th}_{j-1/2} - \widehat{Tc}_{j-1/2})\ \pi\ dte\ NB}\right]\right\} \le \widehat{\Delta P}_{h_{disp}} \quad (72)$$

$$\sum_{j=2}^{J} \frac{-\widehat{\Delta T}_h}{\hat{\rho}_{c,j-1/2}}\left\{\left(\frac{\hat{m}_c}{NB\ As_c}\right)^2 \hat{\beta}_{c,j+1/2}\frac{\hat{m}_h\ \widehat{Cp}_{h,j-1/2}}{\hat{m}_c\ \widehat{Cp}_{c,j-1/2}} + \left(\frac{\hat{m}_c}{NB\ As_c}\right)^2 \frac{f_{c,j-1/2}(NB,\ dti,\ dte,\ Dti)}{2dti}\left[\frac{\hat{m}_h\ \widehat{Cp}_{h,j-1/2}}{U_{j-1/2}(NB,\ dti,\ dte,\ Dti)(\widehat{Th}_{j-1/2} - \widehat{Tc}_{j-1/2})\pi\ dte\ NB}\right]\right\} \le \widehat{\Delta P}_{c_{disp}} \quad (73)$$

The stream flow velocity must be within an acceptable range, which add the following constraints

$$\widehat{v\min}_h \le v_h \le \widehat{v\max}_h \quad (74)$$

$$\widehat{v\min}_c \le v_c \le \widehat{v\max}_c \quad (75)$$

where $\widehat{v\min}$ and $\widehat{v\max}$ are the corresponding lower and upper bounds, respectively. The representation of these constraints in

https://doi.org/10.1021/acs.iecr.1c02455
Ind. Eng. Chem. Res. 2021, 60, 17611−17625

connection with the design variables is presented through the substitution of eqs 10−13 into eqs 74 and 75, which yields

$$\widehat{v\min}_{\mathrm{h}} \le \frac{(\hat{m}_{\mathrm{h}}/\hat{\rho}_{\mathrm{h},j})}{NB\frac{\pi}{4}(Dti^2 - dte^2)} \le \widehat{v\max}_{\mathrm{h}} \quad \text{for } j = 1, ..., J \tag{76}$$

$$\widehat{v\min}_{\mathrm{c}} \le \frac{(\hat{m}_{\mathrm{c}}/\hat{\rho}_{\mathrm{c},j})}{NB\left(\frac{\pi dti^2}{4}\right)} \le \widehat{v\max}_{\mathrm{c}} \quad \text{for } j = 1, ..., J \tag{77}$$

The imposition of turbulent flow yields the following constraints

$$Re_{\mathrm{h}} \ge 4000 \tag{78}$$

$$Re_{\mathrm{c}} \ge 4000 \tag{79}$$

which are equivalent to

$$\frac{4\ dh\ \hat{m}_{\mathrm{h}}}{NB\ \pi(Dti^2 - dte^2)\ \hat{\mu}_{\mathrm{h},j}} \ge 4000 \quad \text{for } j = 1, ..., J \tag{80}$$

$$\frac{4\ \hat{m}_{\mathrm{c}}}{NB\ \pi dti\ \hat{\mu}_{\mathrm{c},j}} \ge 4000 \quad \text{for } j = 1, ..., J \tag{81}$$

Finally, the outer diameter of the inner tube and the inner diameter of the outer tube must obey the following relation

$$Dti \ge dte + \hat{\varepsilon} \tag{82}$$

where $\hat{\varepsilon}$ is the smallest difference between the diameters of the outer and inner tubes.

The number of hairpins connected in series in a unit and the number of parallel branches are a discrete variable by nature. The tube diameters are also discrete variables due to the commercial standardization. Therefore, these variables can be expressed through sets of binary variables associated with the corresponding available discrete values, as follows

$$dti = \sum_{sd=1}^{sd\max} \widehat{pdti}_{sd}\, yd_{sd} \tag{83}$$

$$dte = \sum_{sd=1}^{sd\max} \widehat{pdte}_{sd}\, yd_{sd} \tag{84}$$

$$Dti = \sum_{ss=1}^{sD\max} \widehat{pDti}_{sD}\, yD_{sD} \tag{85}$$

$$Dte = \sum_{ss=1}^{sD\max} \widehat{pDte}_{sD}\, yD_{sD} \tag{86}$$

$$NB = \sum_{sB=1}^{sB\max} \widehat{pNB}_{sB}\, yB_{sB} \tag{87}$$

$$NS = \sum_{sE=1}^{sE\max} \widehat{pNS}_{sE}\, yE_{sE} \tag{88}$$

where yd_{sd} is the binary variable that represents the discrete alternative of the inner and outer diameters of the inner tube, $\widehat{pdti}_{sd}$ and $\widehat{pdte}_{sd}$, associated with the index sd; yD_{sD} is the binary variable that represents the discrete alternative of the inner and outer diameters of the outer tube, $\widehat{pDti}_{sD}$ and $\widehat{pDte}_{sD}$, associated with the index sD; yB_{sB} is the binary variable that represents the alternative of the number of branches $\widehat{pNB}_{sB}$ associated with the index sB; and yE_{sE} is the binary variable that represents the alternative of the number of hairpins in series associated with the index sE.

Since only one discrete alternative must be chosen for each design variable, then

$$\sum_{sd=1}^{sd\max} yd_{sd} = 1 \tag{89}$$

$$\sum_{sD=1}^{sD\max} yD_{sD} = 1 \tag{90}$$

$$\sum_{sB=1}^{sB\max} yB_{sB} = 1 \tag{91}$$

$$\sum_{sE=1}^{sE\max} yE_{sE} = 1 \tag{92}$$

The current form of the optimization problem corresponds to the minimization of eq 66 subject to eqs 67, 72, 73, 76, 77, and 80−92.

Alternatively, the heat exchanger design optimization can also be formulated as the minimization of the total annualized cost, including capital and operating costs. In this case, the constraints related to the pressure drop bounds in eqs 72 and 73 are eliminated and the objective function displayed in eq 66 is substituted by

$$Min\ \mathrm{TAC} = \hat{r}C_{\mathrm{cap}} + C_{\mathrm{op,h}} + C_{\mathrm{op,c}} \tag{93}$$

where TAC is the total annualized cost, C_{cap} is the capital cost, $C_{\mathrm{op,h}}$ and $C_{\mathrm{op,c}}$ are the operating costs in a yearly basis for the hot and cold streams, respectively, and $\hat{r}$ is the annualizing factor. The expression of the annualizing factor is

$$\hat{r} = \frac{\hat{i}(1+\hat{i})^{\hat{n}}}{(1+\hat{i})^{\hat{n}} - 1} \tag{94}$$

where $\hat{i}$ is the interesting rate and $\hat{n}$ is the project horizon in years.

The capital cost can be evaluated by

$$C_{\mathrm{cap}} = \hat{a} + \hat{b}Atot^{\hat{n}} \tag{95}$$

where $\hat{a}$ and $\hat{b}$ are model parameters of the cost correlation. The expression for the evaluation of the energy consumption for each stream is given by

$$C_{\mathrm{op}} = \widehat{Nop}\frac{\widehat{ep}}{10^3}\left(\frac{\Delta P\ \hat{m}}{\hat{\eta}\hat{\rho}}\right) \tag{96}$$

where $\widehat{ep}$ is the energy price, $\hat{m}$ is the mass flow rate (hot or cold), $\hat{\eta}$ is the pump efficiency, $\hat{\rho}$ is the fluid density (hot or cold), and $\widehat{Nop}$ is the number of operating hours per year.

Using the same substitutions that yields eq 66, the capital cost becomes

$$C_{\mathrm{cap}} = \hat{a} + \hat{b}\left(\sum_{j=2}^{J} \frac{-\hat{m}_{\mathrm{h}}\ \widehat{Cp}_{\mathrm{h},j-1/2}\widehat{\Delta T}_{\mathrm{h}}}{U_{j-1/2}(NB,\ dti,\ dte,\ Dti)(\widehat{Th}_{j-1/2} - \widehat{Tc}_{j-1/2})}\right)^{\hat{n}} \tag{97}$$

https://doi.org/10.1021/acs.iecr.1c02455
Ind. Eng. Chem. Res. 2021, 60, 17611−17625

The operational cost can be calculated using the same transformation that yields eqs 72 and 73

$$C_{op,h} = \widehat{Nop}\frac{\widehat{ep}}{10^3}\left(\frac{\widehat{m_h}}{\hat{\eta}\widehat{\rho_h}}\right)\sum_{j=2}^{J}\frac{\widehat{\Delta T_h}}{\hat{\rho}_{h,j-1/2}}\left\{\left(\frac{\hat{m}_h}{NB\ As_h}\right)^2\hat{\beta}_{h,j+1/2} - \left(\frac{\hat{m}_h}{NB\ As_h}\right)^2\frac{\hat{f}_{h,j-1/2}\ (NB,\ dti,\ dte,\ Dti)}{2dh}\left[\frac{\hat{m}_h\ \widehat{Cp}_{h,j-1/2}}{\hat{U}_{j-1/2}(NB,\ dti,\ dte,\ Dti)(\widehat{Th}_{j-1/2} - \widehat{Tc}_{j-1/2})\pi\ dte\ NB}\right]\right\} \tag{98}$$

$$C_{op,c} = \widehat{Nop}\frac{\widehat{ep}}{10^3}\left(\frac{\widehat{m_c}}{\hat{\eta}\widehat{\rho_c}}\right)\sum_{j=2}^{J}\frac{-\widehat{\Delta T_h}}{\hat{\rho}_{c,j-1/2}}\left\{\left(\frac{\hat{m}_c}{NB\ As_c}\right)^2\hat{\beta}_{c,j+1/2}\frac{\widehat{m_h}\ \widehat{Cp}_{h,j-1/2}}{\widehat{m_c}\widehat{Cp}_{c,j-1/2}} + \left(\frac{\hat{m}_c}{NB\ As_c}\right)^2\frac{\hat{f}_{c,j-1/2}\ (NB,\ dti,\ dte,\ Dti)}{2dti}\left[\frac{\hat{m}_h\ \widehat{Cp}_{h,j-1/2}}{\hat{U}_{j-1/2}(NB,\ dti,\ dte,\ Dti)(\widehat{Th}_{j-1/2} - \widehat{Tc}_{j-1/2})\pi\ dte\ NB}\right]\right\} \tag{99}$$

Therefore, the objective function becomes

$$\min\ \hat{a} + \hat{b}\left(\sum_{j=2}^{J}\frac{-\hat{m}_h\ \widehat{Cp}_{h,j-1/2}\widehat{\Delta T_h}}{\hat{U}_{j-1/2}(NB,\ dti,\ dte,\ Dti)(\widehat{Th}_{j-1/2} - \widehat{Tc}_{j-1/2})}\right)^{\hat{n}} + \widehat{Nop}\frac{\widehat{ep}}{10^3}\left(\frac{\widehat{m_h}}{\hat{\eta}\widehat{\rho_h}}\right)\sum_{j=2}^{J}\frac{\widehat{\Delta T_h}}{\hat{\rho}_{h,j-1/2}}\left\{\left(\frac{\hat{m}_h}{NB\ As_h}\right)^2\hat{\beta}_{h,j+1/2} - \left(\frac{\hat{m}_h}{NB\ As_h}\right)^2\frac{\hat{f}_{h,j-1/2}\ (NB,\ dti,\ dte,\ Dti)}{2dh}\left[\frac{\hat{m}_h\ \widehat{Cp}_{h,j-1/2}}{\hat{U}_{j-1/2}(NB,\ dti,\ dte,\ Dti)(\widehat{Th}_{j-1/2} - \widehat{Tc}_{j-1/2})\pi\ dte\ NB}\right]\right\} + \widehat{Nop}\frac{\widehat{ep}}{10^3}\left(\frac{\widehat{m_c}}{\hat{\eta}\widehat{\rho_c}}\right)\sum_{j=2}^{J}\frac{-\widehat{\Delta T_h}}{\hat{\rho}_{c,j-1/2}}\left\{\left(\frac{\hat{m}_c}{NB\ As_c}\right)^2\hat{\beta}_{c,j+1/2}\frac{\widehat{m_h}\ \widehat{Cp}_{h,j-1/2}}{\widehat{m_c}\widehat{Cp}_{c,j-1/2}} + \left(\frac{\hat{m}_c}{NB\ As_c}\right)^2\frac{\hat{f}_{c,j-1/2}\ (NB,\ dti,\ dte,\ Dti)}{2dti}\left[\frac{\hat{m}_h\ \widehat{Cp}_{h,j-1/2}}{\hat{U}_{j-1/2}(NB,\ dti,\ dte,\ Dti)(\widehat{Th}_{j-1/2} - \widehat{Tc}_{j-1/2})\pi\ dte\ NB}\right]\right\} \tag{100}$$

Finally, the optimization problem based on the minimization of TAC corresponds to the objective function displayed in eq 100 subject to the constraints in eqs 67, 76,77, and 80−92.

The design optimization problem based on the minimization of the area or the minimization of the TAC corresponds to a mixed-integer nonlinear programming problem (MINLP). This problem is reformulated to a linear form in the next section.

5. MODEL REFORMULATION

The set of eqs 83−92 corresponds to the so-called discrete representation of the search space of the design variables The alternative description of the search space employed in the current paper corresponds to a combinatorial representation.[22]

The combinatorial representation of the space of discrete independent variables is composed of a single set of binaries, $yrow_{srow}$, associated with the candidate solutions. The index of this variable, srow, is a multi-index encompassing all original indices. Therefore, each element srow identifies a combination of discrete values of the design variables, such that each element srow represents a solution candidate (i.e., a heat exchanger alternative characterized by a set of discrete values of the design variables). In this organization of the search space, eqs 83−92 are substituted by

$$dti = \sum_{srow}\widehat{Pdti}_{srow}yrow_{srow} \tag{101}$$

$$dte = \sum_{srow}\widehat{Pdte}_{srow}yrow_{srow} \tag{102}$$

$$Dti = \sum_{srow}\widehat{PDti}_{srow}yrow_{srow} \tag{103}$$

$$Dte = \sum_{srow}\widehat{PDte}_{srow}yrow_{srow} \tag{104}$$

$$NB = \sum_{srow}\widehat{PNB}_{srow}yrow_{srow} \tag{105}$$

$$NS = \sum_{srow}\widehat{PNS}_{srow}yrow_{srow} \tag{106}$$

$$\sum_{srow}yrow_{srow} = 1 \tag{107}$$

The parameters in eqs 101−106 that represent the discrete values of the design variables are equivalent to the original ones but reorganized according to the new variable indexation. Further details of this alternative representation of the search space can be found in Gonçalves et al.[23]

The heat exchanger discretized model described in the previous section is originally nonlinear, but it is reformulated here to a linear form. The reformulation procedure is based on the substitution of all discrete design variables by the expressions in eqs 101−106 in the corresponding constraints, followed by a reorganization of the resultant mathematical expressions that explore the binary nature of the variables $yrow_{srow}$.

The procedure is illustrated below in relation to the objective function (eq 66). Initially, the substitution of eqs 101−106 into eq 66 yields

$$\min\sum_{srow}\sum_{j=2}^{J}\frac{-\hat{m}_h\ \widehat{Cp}_{h,j-1/2}\widehat{\Delta T_h}}{\hat{U}_{j-1/2,srow}(\widehat{Th}_{j-1/2} - \widehat{Tc}_{j-1/2})}yrow_{srow} + \widehat{ph}\left(\sum_{srow}\widehat{PNB}_{srow}yrow_{srow}\right)\left(\sum_{srow}\widehat{PNS}_{srow}yrow_{srow}\right) \tag{108}$$

Because *yrow* is a binary variable and only one candidate is present in the solution (see eq 107), eq 108 can be reorganized to a linear form as follows

https://doi.org/10.1021/acs.iecr.1c02455
Ind. Eng. Chem. Res. 2021, 60, 17611−17625

$$\min \sum_{\text{srow}} \sum_{j=2}^{J} \left[\frac{-\hat{m}_{\text{h}} \widehat{Cp}_{\text{h},j} \widehat{\Delta T}_{\text{h}}}{\hat{U}_{j-1/2,\text{srow}} \left(\left(\hat{T}_{\text{h},j-1} + \frac{\widehat{\Delta T}}{2} \right) - \left(\hat{T}_{\text{c},j-1} + \frac{\widehat{\Delta T}}{2} \right) \right)} + \widehat{ph}\ \widehat{PNS}_{\text{srow}}\ \widehat{PNB}_{\text{srow}} \right] yrow_{\text{srow}} \tag{109}$$

This procedure can be applied to all constraints, thus resulting in the following linear representation of the optimization problem.

The tube length of hairpin constraints in eq 67 becomes

$$\widehat{Lh}^{\text{LB}} \le \sum_{\text{srow}} \sum_{j=2}^{J} \frac{-\widehat{\Delta T}_{\text{h}} \hat{m}_{\text{h}}\ \widehat{Cp}_{\text{h},j-1/2}}{\hat{U}_{j-1/2,\text{srow}} (\widehat{Th}_{j-1/2} - \widehat{Tc}_{j-1/2}) \pi\ \widehat{Pdte}_{\text{srow}} \widehat{PNB}_{\text{srow}} \widehat{PNS}_{\text{srow}}}$$
$$yrow_{\text{srow}} \le \widehat{Lh}^{\text{UB}} \tag{110}$$

The hot- and cold-stream velocity constraints in eqs 76 and 77 become

$$\widehat{v\text{min}}_{\text{h}} \le \sum_{\text{srow}} \frac{(\hat{m}_{\text{h}}/\hat{\rho}_{\text{h},j})}{\widehat{PNB}_{\text{srow}} \frac{\pi}{4} (\widehat{PDti}_{\text{srow}}{}^2 - \widehat{Pdte}_{\text{srow}}{}^2)} yrow_{\text{srow}}$$
$$\le \widehat{v\text{max}}_{\text{h}} \quad \text{for } j = 1, \ldots, J \tag{111}$$

$$\widehat{v\text{min}}_{\text{c}} \le \sum_{\text{srow}} \frac{4(\hat{m}_{\text{c}}/\hat{\rho}_{\text{c},j})}{\widehat{PNB}_{\text{srow}} \pi \widehat{Pdti}_{\text{srow}}{}^2} yrow_{\text{srow}} \le \widehat{v\text{max}}_{\text{c}}$$
$$\text{for } j = 1, \ldots, J \tag{112}$$

The hot- and cold-stream pressure drop constraints in eqs 72 and 73 are given by

$$\sum_{\text{srow}} \sum_{j=2}^{J} \frac{\widehat{\Delta T}_{\text{h}}}{\hat{\rho}_{\text{h},j-1/2}} \left\{ \left(\frac{\hat{m}_{\text{h}}}{\widehat{PNB}_{\text{srow}}\ \widehat{PAs}_{\text{h,srow}}} \right)^2 \hat{\beta}_{\text{h},j+1/2} - \left(\frac{\hat{m}_{\text{h}}}{\widehat{PNB}_{\text{srow}}\ \widehat{PAs}_{\text{h,srow}}} \right)^2 \frac{\hat{f}_{\text{h},j-1/2,\text{srow}}}{2\ \widehat{pdh}_{\text{srow}}} \left[\frac{\hat{m}_{\text{h}}\ \widehat{Cp}_{\text{h},j-1/2}}{\hat{U}_{j-1/2,\text{srow}} (\hat{T}_{\text{h},j-1/2} - \hat{T}_{\text{c},j-1/2}) \pi\ \widehat{Pdte}_{\text{srow}}\ \widehat{PNB}_{\text{srow}}} \right] \right\}$$
$$yrow_{\text{srow}} \le \widehat{\Delta P}_{\text{h}_{\text{disp}}} \tag{113}$$

$$\sum_{\text{srow}} \sum_{j} \frac{-\widehat{\Delta T}_{\text{h}}}{\hat{\rho}_{\text{c},j-1/2}} \left\{ \left(\frac{\hat{m}_{\text{c}}}{\widehat{PNB}_{\text{srow}}\ \widehat{PAs}_{\text{c,srow}}} \right)^2 \hat{\beta}_{\text{c},j+1/2} \frac{\widehat{m}_{\text{h}}\ \widehat{Cp}_{\text{h},j-1/2}}{\widehat{m}_{\text{c}} \widehat{Cp}_{\text{c},j-1/2}} + \left(\frac{\hat{m}_{\text{c}}}{\widehat{PNB}_{\text{srow}}\ \widehat{PAs}_{\text{c,srow}}} \right)^2 \frac{\hat{f}_{\text{c},j-1/2,\text{srow}}}{2\ \widehat{pdti}_{\text{srow}}} \left[\frac{\hat{m}_{\text{h}}\ \widehat{Cp}_{\text{h},j-1/2}}{\hat{U}_{j-1/2,\text{srow}} (\hat{T}_{\text{h},j-1/2} - \hat{T}_{\text{c},j-1/2}) \pi\ \widehat{Pdte}_{\text{srow}}\ \widehat{PNB}_{\text{srow}}} \right] \right\}$$
$$yrow_{\text{srow}} \le \widehat{\Delta P}_{\text{c}_{\text{disp}}} \tag{114}$$

The Reynolds number constraints in eqs 78 and 79 are given by

$$\sum_{\text{srow}} \frac{4\ \hat{m}_{\text{c}}}{\widehat{PNB}_{\text{srow}}\ \pi\ \widehat{Pdti}_{\text{srow}}\ \hat{\mu}_{\text{c},j-1/2}} yrow_{\text{srow}} \ge 4000$$
$$\text{for } j = 1, \ldots, J \tag{115}$$

$$\sum_{\text{srow}} \frac{\widehat{Pdh}_{\text{srow}}\ \hat{m}_{\text{h}}}{\widehat{PNB}_{\text{srow}}\ \widehat{PAs}_{\text{h,srow}}\ \hat{\mu}_{\text{h},j-1/2}} yrow_{\text{srow}} \ge 4000$$
$$\text{for } j = 1, \ldots, J \tag{116}$$

The same procedure is used to obtain a linear objective function for the minimization of TAC in eq 100, which yields

$$\min \hat{a} + \hat{b} \left(\sum_{\text{srow}} \sum_{j=2}^{J} \left[\frac{-\hat{m}_{\text{h}} \widehat{Cp}_{\text{h},j} \widehat{\Delta T}_{\text{h}}}{\hat{U}_{j-1/2,\text{srow}} \left(\left(\hat{T}_{\text{h},j-1} + \frac{\widehat{\Delta T}}{2} \right) - \left(\hat{T}_{\text{c},j-1} + \frac{\widehat{\Delta T}}{2} \right) \right)} \right] \right)^{\hat{n}}$$
$$yrow_{\text{srow}} + \sum_{\text{srow}} \sum_{j=2}^{J} \frac{\widehat{\Delta T}_{\text{h}}}{\hat{\rho}_{\text{h},j-1/2}} \left\{ \left(\frac{\hat{m}_{\text{h}}}{\widehat{PNB}_{\text{srow}}\ \widehat{PAs}_{\text{h,srow}}} \right)^2 \hat{\beta}_{\text{h},j+1/2} - \left(\frac{\hat{m}_{\text{h}}}{\widehat{PNB}_{\text{srow}}\ \widehat{PAs}_{\text{h,srow}}} \right)^2 \frac{\hat{f}_{\text{h},j-1/2,\text{srow}}}{2\ \widehat{pdh}_{\text{srow}}} \left[\frac{\hat{m}_{\text{h}}\ \widehat{Cp}_{\text{h},j-1/2}}{\hat{U}_{j-1/2,\text{srow}} (\hat{T}_{\text{h},j-1/2} - \hat{T}_{\text{c},j-1/2}) \pi\ \widehat{Pdte}_{\text{srow}}\ \widehat{PNB}_{\text{srow}}} \right] \right\} yrow_{\text{srow}}$$
$$+ \sum_{\text{srow}} \sum_{j} \frac{-\widehat{\Delta T}_{\text{h}}}{\hat{\rho}_{\text{c},j-1/2}} \left\{ \left(\frac{\hat{m}_{\text{c}}}{\widehat{PNB}_{\text{srow}}\ \widehat{PAs}_{\text{c,srow}}} \right)^2 \hat{\beta}_{\text{c},j+1/2} \frac{\widehat{m}_{\text{h}}\ \widehat{Cp}_{\text{h},j-1/2}}{\widehat{m}_{\text{c}} \widehat{Cp}_{\text{c},j-1/2}} + \left(\frac{\hat{m}_{\text{c}}}{\widehat{PNB}_{\text{srow}}\ \widehat{PAs}_{\text{c,srow}}} \right)^2 \frac{\hat{f}_{\text{c},j-1/2,\text{srow}}}{2\ \widehat{pdti}_{\text{srow}}} \left[\frac{\hat{m}_{\text{h}}\ \widehat{Cp}_{\text{h},j-1/2}}{\hat{U}_{j-1/2,\text{srow}} (\hat{T}_{\text{h},j-1/2} - \hat{T}_{\text{c},j-1/2})\ \pi\ \widehat{Pdte}_{\text{srow}}\ \widehat{PNB}_{\text{srow}}} \right] \right\} yrow_{\text{srow}} \tag{117}$$

The final form of the optimization problem represented by the minimization of the area in eq 109 subject to the constraints in eqs 110−116 and by the TAC minimization in eq 117 subject to the constraints in eqs 100−112, 115, and 116 corresponds to an integer linear model (ILM). Because of its linear nature, the solution of this ILM is the global optimum of the design problem. Additionally, the available algorithms to solve ILP problems do not present convergence drawbacks, like those observed in nonlinear problems.

6. RESULTS

The design optimization procedure using the ILM formulation was applied to two design problems proposed in the current paper and solved using integer linear programming (ILP) through the solver CPLEX[24] (version 12.5.1.0) in the software GAMS[25] (version 24.1.3). The hot and cold streams of the problems correspond to an aqueous solution with 70% m/m of ethylene glycol. The mathematical functions that describe the variations of the physical properties of the ethylene glycol solution with the temperature are based on Bohne et al.[26] and are displayed in the Supporting Information.

The search space of the inner and outer tube diameters is presented in Table 2. The options of the number of hairpins in each unit and number of branches correspond to 1−20. Therefore, the combinatorial search space is composed of 32 400 solution candidates (20 × 20 × 9 × 9). This amount corresponds to the number of binary variables of the ILP

https://doi.org/10.1021/acs.iecr.1c02455
Ind. Eng. Chem. Res. 2021, 60, 17611−17625

Table 2. Available Tube Diameters

	inner tube		outer tube	
alternative	inner diameter (m)	outer diameter (m)	inner diameter (m)	outer diameter (m)
1	0.01580	0.02134	0.03505	0.04216
2	0.02093	0.02667	0.04089	0.04826
3	0.02664	0.03340	0.052502	0.06032
4	0.03505	0.04216	0.06271	0.07302
5	0.04089	0.04826	0.07793	0.0889
6	0.05250	0.06032	0.09012	0.1016
7	0.06271	0.07302	0.1023	0.1143
8	0.07793	0.08890	0.1144	0.1270
9	0.09012	0.1016	0.1553	0.1683

problem. The number of constraints is much smaller: 606 for the area minimization and 604 for the TAC minimization.

The lower and upper bounds on the tube lengths are 3.048 and 15.24 m, respectively. The flow velocity must be within 0.65 and 3 m/s. The allowable pressure drop is 0.8 bar for both streams.

Aiming at discussing the importance of modeling the system considering the variation of the physical properties through discretization of the conservation equations, the design problems were also solved assuming uniform values of the physical properties. This assumption is equivalent to the analytical models usually employed in design optimization problems (LMTD and ε-NTU methods) (see Table 1). Two alternatives were considered for the evaluation of the physical properties when using uniform heat transfer coefficient values:

1. Alternative 1 employs physical properties calculated at the average temperature between the inlet and outlet conditions and
2. Alternative 2 utilizes the average of the values of the physical properties evaluated at the inlet and outlet temperatures.

Two design examples were explored, both solved through the minimization of area and TAC. The temperature grid of the discretization procedure applied in all examples was composed of 100 points. The parameter $\widehat{phi}$ in the objective function was equal to 10^{-5}. The Supporting Information contains a sensitivity analysis that shows that this size of the grid is adequate for this problem.

6.1. Area Minimization. Example 1

The data of the design task of this example are displayed in Table 3.

The optimal solutions using the different approaches mentioned above are shown in Table 4.

Table 3. Example 1: Design Task Data

parameter	value
hot-stream inlet temperature, $\widehat{Thi}$ (°C)	95
hot-stream outlet temperature, $\widehat{Tho}$ (°C)	80
cold-stream inlet temperature, $\widehat{Tci}$ (°C)	30
cold-stream outlet temperature, $\widehat{Tco}$ (°C)	47.3
hot-stream mass flow rate, $\widehat{mh}$ (kg/s)	15
cold-stream mass flow rate, $\widehat{mc}$ (kg/s)	14
hot-stream fouling factor, $\widehat{Rfh}$ (m^2 °C/W)	0.0002
cold-stream fouling factor, $\widehat{Rfc}$ (m^2 °C/W)	0.0004

The analysis of the results of example 1 in Table 4 indicates that the optimal heat transfer area calculated using the proposed approach is similar to the values obtained using the optimization with uniform values of the physical properties. This example illustrates a case where models based on analytical solutions provide a satisfactory representation of the heat exchanger behavior.

Example 2

The data of the design task of this example are displayed in Table 5.

The optimal solutions in example 2 using the different approaches mentioned above are shown in Table 6.

Unlike what takes place in example 1, the results of example 2 present remarkably distinct solutions obtained through the set of approaches, as discussed below.

Figures 5 and 6 show the profiles of the spatial coordinate and the overall heat transfer coefficient using the proposed discretized approach. It is important to observe the large variation of the overall heat transfer coefficient along the temperature range in Figure 6, which can explain the difference between the heat transfer area calculated using the proposed approach and the results obtained through the optimization using uniform values of the physical properties.

Figure 7 depicts the pressure profile of the optimal solution in relation to the spatial coordinate. When the physical properties are constant, these profiles are linear, but it is possible to observe in Figure 7 a variation of the pressure gradient of the cold stream along the spatial coordinate due to the variation of the fluid viscosity (the pressure drop decreases along the flow path due to the reduction of the viscosity with the increase of the temperature).

The solution based on Alternative 1 attains a smaller heat transfer area than the proposed approach. However, it is important to check the performance of this solution using the rigorous modeling presented in the proposed procedure. Therefore, the solution obtained using Alternative 1 was evaluated using the set of equations of the discretized model with variable physical properties (eqs 29 and 30). The results are displayed in Figure 8, which depicts the total required tube length along the temperature grid. The mark in the y-axis represents the total length of all hairpins in series associated with Alternative 1 solution, 55.42 m, which is lower than the required length, 58.21 m, thus indicating that this solution is unfit for the thermal task according to the rigorous model.

The reason for the total tube length obtained using Alternative 1 to be infeasible for the design task can be illustrated by the profiles of the overall heat transfer coefficient displayed in Figure 9. The solid line corresponds to the analysis using variable physical properties, and the dashed line is the uniform value of the overall heat transfer coefficient employed in Alternative 1. The mean value of the overall heat transfer coefficient profile calculated using the proposed approach is 515 W/(m^2 °C), and the uniform value employed in the design of Alternative 1 is 527 W/(m^2 °C), i.e., the simplified assumption in Alternative 1 of uniform values of physical properties overestimates the overall heat transfer coefficient, which implied an undersized heat exchanger.

The infeasibility of the solution obtained using Alternative 1 was already expected because the optimal solution obtained using the proposed approach is global (the optimization problem is linear); thus, any other solution with a lower heat transfer area is not feasible.

https://doi.org/10.1021/acs.iecr.1c02455
Ind. Eng. Chem. Res. 2021, 60, 17611−17625

Table 4. Area Minimization—Example 1: Optimal Double-Pipe Heat Exchangers

approach	inner tube alternative	outer tube alternative	number of hairpins	number of branches	total length (m)	heat transfer area (m^2)
uniform physical properties alternative 1	7	7	3	2	15.17	20.88
uniform physical properties alternative 2	7	7	4	2	11.50	21.09
proposed discretized approach	7	7	3	2	15.20	20.92

Table 5. Example 2: Design Task Data

parameter	value
hot-stream inlet temperature, $\widehat{Thi}$ (°C)	100
hot-stream outlet temperature, $\widehat{Tho}$ (°C)	80
cold-stream inlet temperature, $\widehat{Tci}$ (°C)	−10
cold-stream outlet temperature, $\widehat{Tco}$ (°C)	40.5
hot-stream mass flow rate, $\widehat{mh}$ (kg/s)	15
cold-stream mass flow rate, $\widehat{mc}$ (kg/s)	6.7
hot-stream fouling factor, $\widehat{Rfh}$ (m^2 °C/W)	0.0002
cold-stream fouling factor, $\widehat{Rfc}$ (m^2 °C/W)	0.0004

The solution based on Alternative 2 obtains a higher heat transfer area than the proposed approach. The analysis of the heat exchanger obtained through Alternative 2 using the discretized model with variable physical properties (eqs 29 and 30) is displayed in Figure 10. The total length of all hairpins in series associated with Alternative 2 solution, 88.1 m, marked in the *y*-axis, is almost 20% higher than the required length calculated using the rigorous modeling, 73.5 m, which indicates a considerable oversize associated with this heat exchanger.

The motivation of the larger heat transfer area calculated using Alternative 2 is directly associated with the profiles of the overall heat transfer coefficient displayed in Figure 11. The overall heat transfer coefficient calculated at each point of this heat exchanger is above the uniform value calculated using Alternative 2 along almost the entire heat transfer surface. The mean value of the overall heat transfer coefficient calculated using the rigorous modeling is 488 W/(m^2 °C), and the uniform value calculated using Alternative 2 is 398 W/(m^2 °C), which indicates that the adoption of Alternative 2 was associated with an underestimation of the overall heat transfer coefficient, which brought an unnecessary larger heat transfer surface.

6.2. TAC Minimization. The data of the design task of both examples are the same as those of the area minimization problem (Tables 3 and 5). The parameters $\hat{a}$, $\hat{b}$, and $\hat{n}$ for the evaluation of the capital cost are equal to 1900, 2500, and 1, respectively.[27] The energy price is 0.1 $/kWh, the pump efficiency is 0.6, the interest rate is 0.1 for a project horizon of 10 years, and the number of operating hours per year is 8000 h/year.

The optimal solutions in examples 1 and 2 for the TAC minimization using the different approaches mentioned above are shown in Tables 7 and 8.

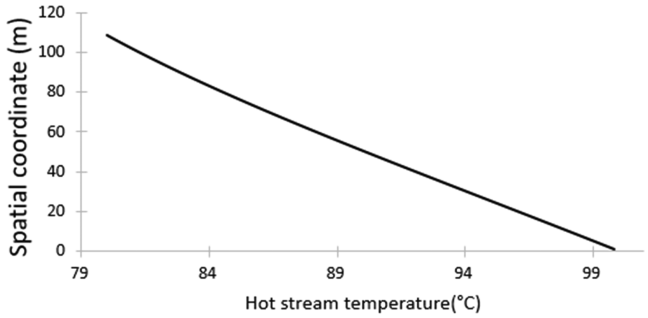

Figure 5. Area minimization—Example 2: required total tube length vs temperature for the discretized model.

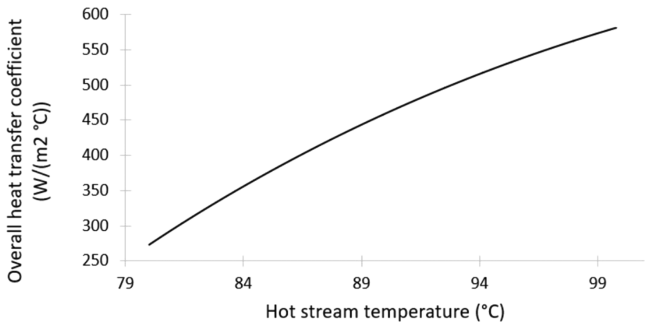

Figure 6. Area minimization—Example 2: overall heat transfer coefficient profiles of the solution obtained using the discretized model.

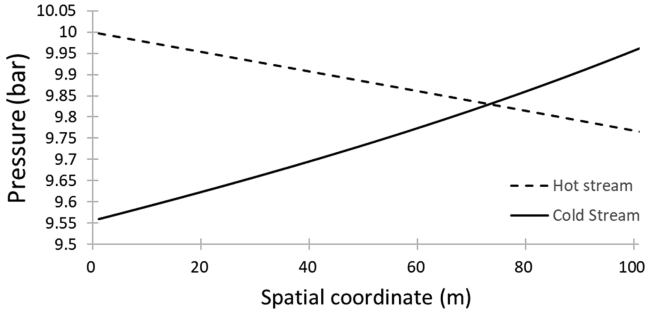

Figure 7. Area minimization—Example 2: pressure profiles of the solution obtained using the discretized model.

Table 6. Area Minimization—Example 2: Optimal Double-Pipe Heat Exchangers

approach	inner tube alternative	outer tube alternative	number of hairpins	number of branches	total length (m)	heat transfer area (m^2)
uniform physical properties alternative 1	5	5	4	3	13.90	25.30
uniform physical properties alternative 2	6	7	6	2	14.73	33.51
proposed discretized approach	8	9	8	1	13.56	30.30

https://doi.org/10.1021/acs.iecr.1c02455
Ind. Eng. Chem. Res. 2021, 60, 17611−17625

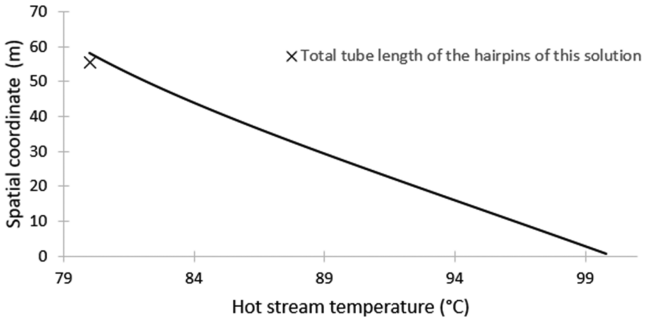

Figure 8. Area minimization—Example 2: required total tube length vs temperature for Alternative 1.

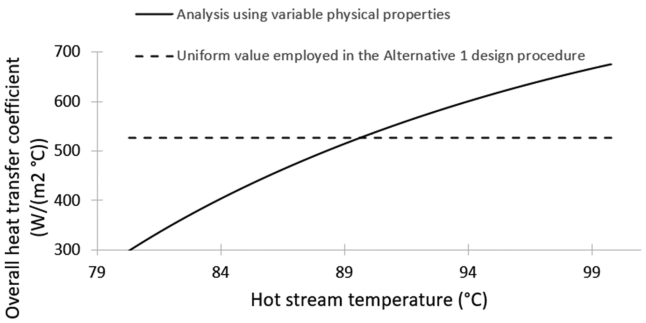

Figure 9. Area minimization—Example 2: overall heat transfer coefficient profiles of the solution obtained using Alternative 1.

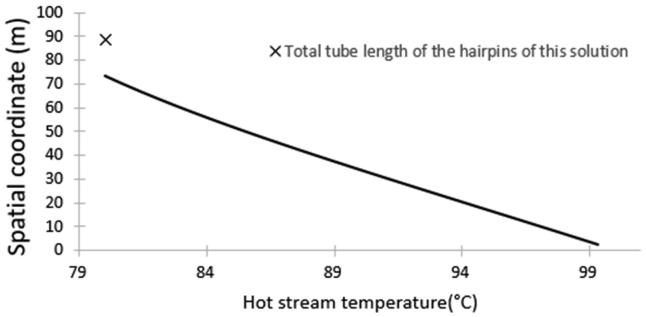

Figure 10. Area minimization—Example 2: required total tube length vs temperature for Alternative 2.

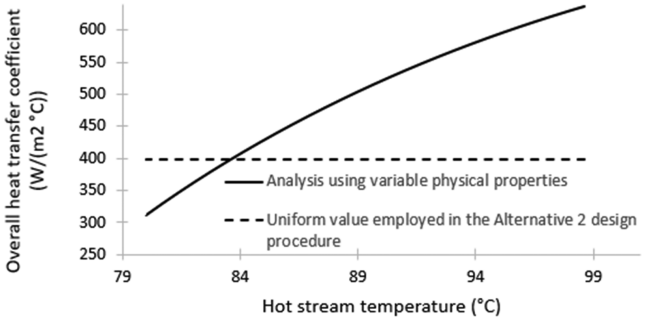

Figure 11. Area minimization—Example 2: overall heat transfer coefficient profiles of the solution obtained using Alternative 2.

The solution behavior obtained in examples 1 and 2 is similar to those obtained in the area minimization problem. For example 1, the total annualized cost and discrete variables are similar for all approaches. In example 2, Alternatives 1 and 2 found, respectively, a smaller and a higher cost solution compared to the proposed approach.

6.3. Comparison between Examples 1 and 2. The difference between the optimal solutions of the proposed approach and those procedures using uniform values of the physical properties is relevant for example 2, but it is not significant for example 1. The reason for this dichotomy can be explained by Figure 12, which shows the variation of the viscosity of the cold stream with temperature.

It is important to observe that the variation of the cold-stream viscosity in example 2 is much higher than the corresponding variation in example 1. Therefore, the approaches based on uniform values of the physical properties fail in the design problem of example 2 but provide satisfactory results in example 1.

6.4. Computational Effort. The computational times employed to solve examples 1 and 2 using different objective functions are displayed in Table 9. These values are associated with a PC computer with a processor i7-8565U 1.8 GHz and an 8 GB RAM memory. The elapsed time is the time consumed from the start of the optimization until its end. The solver time is the time consumed by the CPLEX solver only. The large difference between the elapsed time and the solver time can be explained by the large set of model parameters that must be calculated due to the discretization procedure.

7. CONCLUSIONS

This paper presents the application of an integer linear programming (ILP) formulation for the design of double-pipe heat exchangers. The heat exchanger model is based on the discretization of the conservation equations; therefore, the physical properties are locally evaluated and its variation with temperature is included in the model.

The discretization procedure is based on a temperature grid instead of a conventional spatial one, which allows the calculation of the physical properties before the optimization. Therefore, the nonlinearities associated with the variation of the physical properties with temperature are avoided in the optimization problem. Despite this organization of the optimization problem, the resultant mathematical problem is still nonlinear. However, the adoption of proper techniques allows a reformulation of the design optimization to a linear form. The solution of the ILP problem is always the global optimum and does not present obstacles to convergence, as it occurs in nonlinear formulations.

Comparisons of the proposed approach with two optimization alternatives that consider uniform values of the physical properties indicate that these simplified approaches may yield undersized or oversized solutions when analyzed using the more accurate model that evaluates the physical properties at each point along the grid. The assumption of uniform values of the physical properties is adopted in the analytical methods for the evaluation of heat exchangers usually employed in design optimization problems (e.g., LMTD and ε-NTU). Therefore, it is important to consider the utilization of more accurate modeling for the optimal design of heat exchangers, particularly when the hot or cold streams are associated with large variations of the physical properties with the temperature.

The proposed analysis of the heat exchanger model based on a temperature grid for the equipment design is a flexible approach, which can also be adapted to phase-change streams. If the stream pressure variation is not significant, the proposed approach can be applied based on the vaporization/condensation curves that are evaluated at each temperature along the grid prior to the optimization.

https://doi.org/10.1021/acs.iecr.1c02455
Ind. Eng. Chem. Res. 2021, 60, 17611−17625

Table 7. TAC Minimization—Example 1: Optimal Double-Pipe Heat Exchangers

approach	inner tube alternative	outer tube alternative	number of hairpins	number of branches	total length (m)	heat transfer area (m^2)	TAC ($/year)
uniform physical properties alternative 1	6	6	6	3	6.29	21.46	10 403.61
uniform physical properties alternative 2	6	6	10	3	3.81	21.68	10 517.70
proposed discretized approach	6	6	6	3	6.30	21.51	10 427.43

Table 8. TAC Minimization—Example 2: Optimal Double-Pipe Heat Exchangers

approach	inner tube alternative	outer tube alternative	number of hairpins	number of branches	total length (m)	heat transfer area (m^2)	TAC ($/year)
uniform physical properties alternative 1	5	6	10	2	7.07	21.44	11 481.99
uniform physical properties alternative 2	5	7	8	2	11.01	26.73	13 795.78
proposed discretized approach	6	8	13	1	8.02	19.77	12 175.13

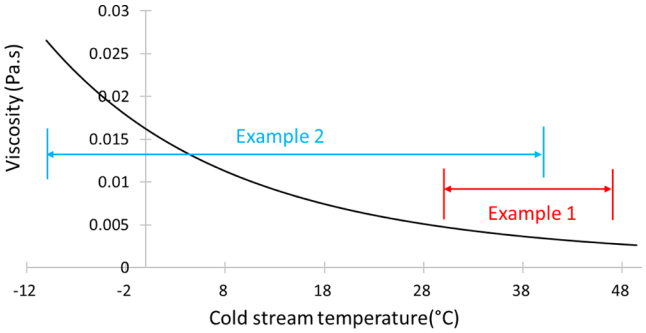

Figure 12. Variation of the viscosity of the ethylene glycol solution with temperature.

Table 9. Computational Times

objective function	example	elapsed time (s)	solver time (s)
area	1	386	14
area	2	399	21
TAC	1	393	19
TAC	2	397	17

■ ASSOCIATED CONTENT

Supporting Information

The Supporting Information is available free of charge at https://pubs.acs.org/doi/10.1021/acs.iecr.1c02455.

Convective heat transfer coefficient and friction factor; thermofluid dynamic properties of the ethylene glycol aqueous solution; and sensitivity analysis of the number of discretization points (PDF)

■ AUTHOR INFORMATION

Corresponding Author

André L. H. Costa − *Rio de Janeiro State University (UERJ), CEP 20550-900 Rio de Janeiro, RJ, Brazil;* orcid.org/0000-0001-9167-8754; Email: andrehc@uerj.br

Authors

André L. M. Nahes − *Rio de Janeiro State University (UERJ), CEP 20550-900 Rio de Janeiro, RJ, Brazil*

Miguel J. Bagajewicz − *School of Chemical, Biological and Materials Engineering, University of Oklahoma, Norman, Oklahoma 73019, United States; Chemistry School, Federal University of Rio de Janeiro (UFRJ), Rio de Janeiro, RJ 21941-909, Brazil;* orcid.org/0000-0003-2195-0833

Complete contact information is available at: https://pubs.acs.org/10.1021/acs.iecr.1c02455

Notes

The authors declare no competing financial interest.

■ ACKNOWLEDGMENTS

A.L.H.C. thanks the National Council for Scientific and Technological Development (CNPq) for the research productivity fellowship (process 310390/2019-2) and the financial support of the Prociência Program (UERJ). M.J.B. thanks the scholarship of visiting researcher from UERJ and the financial support from UFRJ where he is now a visiting professor.

■ NOMENCLATURE

$\widehat{Aexc}$	excess area (%)
A_s	stream cross-sectional area (m^2)
C_{cap}	capital cost ($)
C_{op}	operating costs ($/year)
$\widehat{Cp}$	heat capacity (J/(kg °C))
dh	hydraulic diameter (m)
dte	inner tube external diameter (m)
Dte	outer tube external diameter (m)
dti	inner tube internal diameter (m)
Dti	outer tube internal diameter (m)
$\widehat{ep}$	energy price ($/kWh)
F	mechanical energy loss (J/kg)
$\hat{f}$	friction factor (dimensionless)
$\hat{h}$	convective heat transfer coefficient (W/(m^2 °C))
$\hat{J}$	number of points of the mesh
$\hat{k}$	thermal conductivity (W/(m°C))
L_h	hairpin length (m)
$\hat{m}$	mass flow rate (kg/s)
NB	number of parallel branches
$\widehat{Nop}$	number of operating hours per year (h/year)
NS	number of hairpins in series
$\widehat{Nu}$	Nusselt number (dimensionless)
P	pressure (Pa)
$\widehat{pdti}$	available inner tube internal diameters (m)
$\widehat{pDti}$	available outer tube internal diameters (m)

$\widehat{Pdti}$ inner tube internal diameters of the candidates in the combinatorial search space (m)
$\widehat{PDti}$ outer tube internal diameters of the candidates in the combinatorial search space (m)
$\widehat{pdte}$ available inner tube external diameters (m)
$\widehat{pDte}$ available outer tube external diameters (m)
$\widehat{Pdte}$ inner tube external diameters of the candidates in the combinatorial search space (m)
$\widehat{PDte}$ outer tube external diameters of the candidates in the combinatorial search space (m)
$\widehat{ph}$ penalty factor
$\widehat{pNB}$ number of available branches
$\widehat{PNB}$ number of available branches of the candidates in the combinatorial search space
$\widehat{pNS}$ number of available heat exchangers in series by branch
$\widehat{PNS}$ number of available heat exchangers in series per branch of the candidates in the combinatorial search space
$\hat{r}$ annualizing factor ($year^{-1}$)
$\widehat{Pr}$ Prandtl number (dimensionless)
$\widehat{Re}$ Reynolds number (dimensionless)
$\widehat{Rf}$ fouling resistance (m^2 °C/W)
T temperature (°C)
TAC Total annualized cost ($/year)
$\widehat{Tci}$ cold-stream inlet temperature (°C)
$\widehat{Tco}$ cold-stream outlet temperature (°C)
$\widehat{Thi}$ hot-stream inlet temperature (°C)
$\widehat{Tho}$ hot-stream outlet temperature (°C)
$\hat{U}$ overall heat transfer coefficient (W/(m^2 °C))
v flow velocity (m/s)
yB_{sB} binary variable related with the number of branch selection
yd_{sd} binary variable related with the inner tube diameter selection
yD_{sD} binary variable related with the outer tube diameter selection
yE_{sE} binary variable related with the number of hairpins in series selection
$yrow$ binary variable related with the candidate selection
z spatial coordinate (m)
ΔP pressure drop (Pa)
$\widehat{\Delta P}_{disp}$ allowable stream pressure drop (Pa)
$\widehat{\Delta T}_h$ step size of the mesh (°C)

Greekletters

$\hat{\beta}$ coefficient of thermal expansion (K^{-1})
$\hat{\varepsilon}$ smallest difference between the diameters of the outer and inner tubes (m)
$\hat{\mu}$ dynamic viscosity (Pa·s)
ξ mass fraction of the glycol in the solution
$\hat{\rho}$ density (kg/m^3)
$\hat{\eta}$ pump efficiency

Subscripts

c cold stream
h hot stream
j index of the grid point
sB index of the number of branch selection
sd index of the inner tube diameter selection
sD index of the outer tube diameter selection
sE index of the number of units per branch selection
srow index of the candidates of the combinatorial search space
tube tube material

Superscripts

LB lower bound
UB upper bound

REFERENCES

(1) Rao, R. V.; Saroj, A. Constrained economic optimization of shell-and-tube heat exchangers using elitist-Jaya algotirhm. *Energy* **2017**, *128*, 785−800.
(2) Khosravi, R.; Khosravi, A.; Nahavandi, S.; Hajabdollahi, H. Effectiveness of evolutionary algorithms for optimization of heat exchangers. *Energy Convers. Manage.* **2015**, *89*, 281−288.
(3) Peccini, A.; Lemos, J. C.; Costa, A. L. H.; Bagajewicz, M. J. Optimal design of double pipe heat exchanger structures. *Ind. Eng. Chem. Res.* **2019**, *58*, 12080−12096.
(4) Söylemez, M. S. Thermoeconomical optimization of double-pipe heat exchanger for waste heat recovery. *J. Thermophys. Heat Transfer* **2004**, *18*, 559−563.
(5) Manassaldi, J. I.; Scenna, N. J.; Mussati, S. F. Optimization mathematical model for the detailed design of air cooled heat exchangers. *Energy* **2014**, *64*, 734−746.
(6) Kashani, A. H. A.; Maddahi, A.; Hajabdollahi, H. Thermal-economic optimization of an air-cooled heat exchanger unit. *Appl. Therm. Eng.* **2013**, *54*, 43−55.
(7) Nahes, A. L. M.; Martins, N. R.; Bagajewicz, M. J.; Costa, A. L. H. Computational study of the use of set trimming for the globally optimal design of gasketed-plate heat exchangers. *Ind. Eng. Chem. Res.* **2021**, *60*, 1746−1755.
(8) Raja, B. D.; Jhala, R. L.; Patel, V. Thermal-hydraulic optimization of plate heat exchanger: A multi-objective approach. *Int. J. Therm. Sci.* **2018**, *124*, 522−535.
(9) Peng, H.; Ling, X. Optimal design approach for the plate-fin heat exchangers using neural networks cooperated with genetic algorithms. *Appl. Therm. Eng.* **2008**, *28*, 642−650.
(10) Zarea, H.; Kashkooli, F. M.; Soltani, M.; Rezaeian, M. A novel single and multi-objective optimization approach based on Bees Algorithm Hybrid with Particle Swarm Optimization (BAHPSO): Application to thermal-economic design of plate fin heat exchangers. *Int. J. Therm. Sci.* **2018**, *129*, 552−564.
(11) Mota, F. A. S.; Ravagnani, M. A. S. S.; Carvalho, E. P. Optimal design of plate heat exchangers. *Appl. Therm. Eng.* **2014**, *63*, 33−39.
(12) Short, M.; Isafiade, A. J.; Fraser, D. M.; Kravanja, Z. Synthesis of heat exchanger networks using mathematical programming and heuristics in a two-step optimization procedure with detailed exchanger design. *Chem. Eng. Sci.* **2016**, *144*, 372−385.
(13) Bergman, T. L.; Levine, A. S. *Fundamentals of Heat and Mass Transfer*, 8th ed.; Wiley, 2017.
(14) Bennett, C. A.; Kistler, R. S.; Lestina, T. G. Improving heat exchanger designs. *Heat. Transfer Res.* **2007**, *103*, 40−45.
(15) Parikshit, B.; Spandana, K. R.; Krishna, V.; Seetharam, T. R.; Seetharamu, K. N. A simple method to calculate shell side fluid pressure drop in a shell and tube heat exchanger. *Int. J. Heat Mass Transfer* **2015**, *84*, 700−712.
(16) Pal, E.; Kumar, I.; Joshi, J. B.; Maheshwari, N. K. CFD simulations of shell-side flow in a shell-and-tube type heat exchanger with and without baffles. *Chem. Eng. Sci.* **2016**, *143*, 314−340.
(17) Kazi, S. R.; Short, M.; Biegler, L. T. Heat exchanger network synthesis with detailed exchanger designs: Part 1. A discretized differential algebraic equation model for shell and tube heat exchanger design. *AIChE J.* **2021**, *67*, No. e17056.
(18) Kazi, S. R.; Short, M.; Isafiade, A. J.; Biegler, L. T. Heat exchanger network synthesis with detailed exchangerdesigns - 2. Hybrid optimization strategy for synthesis of heat exchanger networks. *AIChE J.* **2021**, *67*, No. e17057.
(19) Kazi, S. R.; Short, M.; Biegler, L. T. A trust region framework for heat exchanger network synthesis with detailed individual heat exchanger designs. *Comput. Chem. Eng.* **2021**, *153*, No. 107447.

https://doi.org/10.1021/acs.iecr.1c02455
Ind. Eng. Chem. Res. 2021, 60, 17611−17625

(20) Costa, A. L. H.; Bagajewicz, M. J. 110th Anniversary: on the departure from heuristics and simplified models toward globally optimal design of process equipment. *Ind. Eng. Chem. Res.* **2019**, *58*, 18684−18702.
(21) Saunders, E. A. D. *Heat Exchangers Selection, Design and Construction*; John Wiley & Sons: New York, 1988.
(22) Pereira, I. P. S.; Bagajewicz, M. J.; Costa, A. L. H. Global optimization of the design of horizontal shell and tube condensers. *Chem. Eng. Sci.* **2021**, *236*, No. 116474.
(23) Gonçalves, C. O.; Costa, A. L. H.; Bagajewicz, M. J. Alternative MILP formulations for shell and tube heat exchanger optimal design. *Ind. Eng. Chem. Res.* **2017**, *56*, 5970−5979.
(24) CPLEX 12, https://www.gams.com/33/docs/S_CPLEX.html, 2021.
(25) Boisvert, R. F.; Howe, S. E.; Kahaner, D. K. GAMS: a framework for the management of scientific software. *ACM Trans. Math. Software* **1985**, *11*, 313−355.
(26) Bohne, D.; Fischer, S.; Obermeier, E. M. Thermal conductivity, density, viscosity, and Prandtl-numbers of ethylene glycol-water mixtures. *Ber. Bunsen-Ges. Phys. Chem.* **1984**, *88*, 739−742.
(27) Towler, G. T.; Sinnot, R. *Chemical Engineering Design - Principles, Practice and Economics of Plant and Process Design*, 2nd ed.; Butterworth-Heinemann, 2012.

https://doi.org/10.1021/acs.iecr.1c02455
Ind. Eng. Chem. Res. 2021, 60, 17611−17625